

# LY-294002-inhibitable PI 3-kinase and regulation of baseline rates of Na<sup>+</sup> transport in A6 epithelia

TEODOR G. PĂUNESCU,<sup>1</sup> BONNIE L. BLAZER-YOST,<sup>2</sup> CHRIS J. VLAHOS,<sup>3</sup> AND SANDY I. HELMAN<sup>1</sup>

<sup>1</sup>Department of Molecular and Integrative Physiology, University of Illinois at Urbana-Champaign, Urbana, Illinois 61801; <sup>2</sup>Department of Biology, Indiana University-Purdue University at Indianapolis, Indianapolis 46202; and <sup>3</sup>Cardiovascular Research, Lilly Research Laboratories, Eli Lilly and Company, Indianapolis, Indiana 46285

Received 31 August 1999; accepted in final form 23 February 2000

**Păunescu, Teodor G., Bonnie L. Blazer-Yost, Chris J. Vlahos, and Sandy I. Helman.** LY-294002-inhibitable PI 3-kinase and regulation of baseline rates of Na<sup>+</sup> transport in A6 epithelia. *Am J Physiol Cell Physiol* 279: C236–C247, 2000.—Blocker-induced noise analysis of epithelial Na<sup>+</sup> channels (ENaCs) was used to investigate how inhibition of an LY-294002-sensitive phosphatidylinositol 3-kinase (PI 3-kinase) alters Na<sup>+</sup> transport in unstimulated and aldosterone-prestimulated A6 epithelia. From baseline Na<sup>+</sup> transport rates ( $I_{Na}$ ) of  $4.0 \pm 0.1$  (unstimulated) and  $9.1 \pm 0.9$   $\mu\text{A}/\text{cm}^2$  (aldosterone), 10  $\mu\text{M}$  LY-294002 caused, following a relatively small initial increase of transport, a completely reversible inhibition of transport within 90 min to  $33 \pm 6\%$  and  $38 \pm 2\%$  of respective baseline values. Initial increases of transport could be attributed to increases of channel open probability ( $P_o$ ) within 5 min to  $143 \pm 17\%$  (unstimulated) and  $142 \pm 10\%$  of control (aldosterone) from baseline  $P_o$  averaging near 0.5. Inhibition of transport was due to much slower decreases of functional channel densities ( $N_T$ ) to  $28 \pm 4\%$  (unstimulated) and  $35 \pm 3\%$  (aldosterone) of control at 90 min. LY-294002 (50  $\mu\text{M}$ ) caused larger but completely reversible increases of  $P_o$  ( $215 \pm 38\%$  of control at 5 min) and more rapid but only slightly larger decreases of  $N_T$ . Basolateral exposure to LY-294002 induced no detectable effect on transport,  $P_o$  or  $N_T$ . We conclude that an LY-294002-sensitive PI 3-kinase plays an important role in regulation of transport by modulating  $N_T$  and  $P_o$  of ENaCs, but only when presented to apical surfaces of the cells.

epithelial sodium channels; noise analysis; electrophysiology; kidney; cortical collecting ducts; A6 cell line

PHOSPHATIDYLIOSITOL 3-KINASES (PI 3-kinases) catalyze the phosphorylation of the inositol head group of phosphoinositides at the D-3 position (7), generating lipids involved in receptor-mediated signal transduction pathways and membrane trafficking (39). The catalytic activity of PI 3-kinases can be inhibited both in vitro and in vivo by two structurally unrelated compounds, wortmannin and 2-(4-morpholinyl)-8-phenyl-4H-1-benzopyran-4-one (LY-294002) (31, 40). Whereas wortmannin may also inhibit other kinases (11, 28), includ-

ing some members of the PI 4-kinase family (27), LY-294002 was found to have no effect on other ATP-requiring enzymes including PI 4-kinase and protein kinases A and C (40). In contrast to wortmannin, LY-294002 is a highly specific and, importantly, reversible inhibitor for PI 3-kinases that acts as a competitive inhibitor for the ATP binding site of the enzyme with an  $\text{IC}_{50}$  at low micromolar concentrations (40).

There has been considerable recent interest in understanding the involvement of PI 3-kinases in a variety of cellular processes including constitutive and ligand-stimulated vesicular membrane traffic processes (8, 12, 16, 24, 33, 36–38). In particular, PI 3-kinase was shown to be involved in hormone-mediated transmembrane transport phenomena associated with insulin-stimulated insertion of the GLUT-4 glucose transporter into the cell membrane of adipocytes and rat skeletal muscle (9, 13, 42) and in the synthesis and insertion by vesicle trafficking of A-type K<sup>+</sup> channels into the plasma membranes of hippocampal pyramidal neurons (41).

Previous work from our laboratories has shown that PI 3-kinase is required for insulin-mediated Na<sup>+</sup> entry by way of highly selective apical membrane epithelial sodium channels (ENaCs) in A6 epithelia derived from the renal distal tubule of *Xenopus laevis* (31). Recently, we found also that PI 3-kinase activity is required for aldosterone-stimulated Na<sup>+</sup> transport in cultured A6 epithelial cells that exhibit these highly Na<sup>+</sup>-selective apical membrane channels with the same characteristics as those of native tissues (5, 30, 32) and those expressed in oocytes (34). LY-294002 applied apically to A6 epithelia causes a reduction in the density of open ENaCs within the apical membrane of the cells, thus inhibiting Na<sup>+</sup> transport in this model tissue (5). In this regard, it became of interest to know whether the effect of LY-294002 on open-channel density was due to modulation of functional channel densities and/or channel open probabilities of the ENaCs.

Address for reprint requests and other correspondence: S. I. Helman, Dept. of Molecular and Integrative Physiology, 524 Burrill Hall, 407 South Goodwin Ave., Univ. of Illinois at Urbana-Champaign, Urbana, Illinois 61801 (E-mail: s-helman@uiuc.edu).

The costs of publication of this article were defrayed in part by the payment of page charges. The article must therefore be hereby marked "advertisement" in accordance with 18 U.S.C. Section 1734 solely to indicate this fact.

We have used a noninvasive pulse method of weak blocker-induced noise analysis to monitor the time-dependent changes of single-channel currents ( $i_{\text{Na}}$ ), apical membrane functional channel densities ( $N_{\text{T}}$ ), and channel open probabilities ( $P_{\text{o}}$ ) that algebraically determine the net effect of LY-294002 on macroscopic rates of Na<sup>+</sup> transport ( $I_{\text{Na}}$ ). We observed and report that LY-294002 acts exclusively from the apical surface of the cells with entirely different  $P_{\text{o}}$  and  $N_{\text{T}}$  response times. Whereas  $P_{\text{o}}$  is increased almost immediately ( $\sim 1$  min), the decreases of  $N_{\text{T}}$  occurred relatively slowly over 60–90 min, resulting in a completely reversible inhibition of basal rates of Na<sup>+</sup> transport in unstimulated and aldosterone-prestimulated A6 epithelia.

## MATERIALS AND METHODS

**Tissues.** A6 cells were used at passages 115 and 118 and grown in a humidified incubator at 28°C containing 1% CO<sub>2</sub>. The cells were transferred from their frozen state, seeded and grown on 75-cm<sup>2</sup> plastic culture flasks (Costar, Cambridge, MA), and then subcultured on Transwell-Clear cluster inserts (Costar) for at least 10 days to achieve confluence and complete development of their transepithelial transport characteristics (19). The cells were fed twice a week with growth medium that was based in most cases on a mixture of equal parts of Ham's nutrient mixture F-12 with L-glutamine and without sodium bicarbonate (N-6760; Sigma Chemical, St. Louis, MO) and L-15 Leibovitz medium (L-4386, Sigma Chemical). This mixture was supplemented with 10% defined fetal bovine serum (FBS) (SH0070; Hyclone, Logan, UT), 2.57 mM sodium bicarbonate (E. K. Industries, Addison, IL), 3.84 mM L-glutamine (G-7513, Sigma Chemical), 96 U/ml penicillin, and 96 μg/ml streptomycin (17-710R; BioWhittaker, Walkersville, MD). A few tissues were fed with DMEM growth medium (91-5055EC; GIBCO BRL, Grand Island, NY) supplemented with 10% defined FBS, 25 U/ml penicillin, and 25 μg/ml streptomycin. Our laboratories have not observed differences in results between passages 76 and 123.

A6 tissues were short-circuited for the duration of the experiments in edge damage-free chambers (1) and continuously perfused with growth medium without FBS and glutamine at flow rates of  $\sim 7$  ml/min through chamber volumes of  $\sim 0.5$  ml. The short-circuit currents ( $I_{\text{sc}}$ ) were allowed to stabilize for 1.5 h before the start of 2-h control periods, during which time tissues were subjected to noise analysis to establish the baseline parameters of the tissues before challenge with LY-294002.

To compare the effects of LY-294002 in tissues with different baseline rates of Na<sup>+</sup> transport, A6 epithelia were studied in both their unstimulated and aldosterone-prestimulated states (0.27 μM, overnight). LY-294002 was used at concentrations of 10 and 50 μM. An IC<sub>50</sub> of 1.4 μM was reported for both direct in vitro and in vivo inhibition of PI 3-kinase (40), and a half-maximal concentration near 6 μM was required for inhibition of basal and insulin-stimulated macroscopic rates of Na<sup>+</sup> transport in A6 epithelia (31). The experiments were carried out at ambient room temperature.

**Electrical measurements.** The methods of study of amiloride-sensitive ENaCs using blocker-induced noise analysis were identical to those of previous reports from our laboratory (4, 15, 20). The pulse method relies on the fact that weak Na<sup>+</sup> channel blockers like 6-chloro-3,5-diamino-pyrazine-2-carboxamide (CDPC; 27,788-6; Aldrich Chemical, Milwaukee, WI) interact with open channels, causing fluctuations of

the channels between open and blocked states and thereby giving rise to blocker-induced current noise characterized by Lorentzians in power density spectra (PDS) (18, 20). The apical chambers were perfused continuously with solution containing 10 μM CDPC except during pulse intervals, when the CDPC concentration was increased to 30 μM. In these experiments, the 100 μM amiloride-insensitive currents measured at the ends of the experiments averaged near 0.1 μA/cm<sup>2</sup>. After subtraction of the amiloride-insensitive currents from the  $I_{\text{sc}}$ , the macroscopic blocker or amiloride-sensitive Na<sup>+</sup> currents at 10 ( $I_{\text{Na}}^{10}$ ) and 30 μM CDPC ( $I_{\text{Na}}^{30}$ ) were used in all calculations.

Current noise PDS were always measured in pairs at 10 and 30 μM CDPC, giving rise to blocker-induced Lorentzians and fractional inhibitions of the amiloride-sensitive Na<sup>+</sup> currents that were used in calculation of  $i_{\text{Na}}$ ,  $P_{\text{o}}$ , and  $N_{\text{T}}$  at the time points of measurement. The PDS were fit by nonlinear regression (TableCurve 2D; Jandel Scientific, San Rafael, CA) to a mathematical model consisting of low-frequency  $1/f$  noise characterized by the coefficient  $S_1$  and the exponent  $\alpha$  as  $S_1/f^\alpha$ , the blocker-induced Lorentzian characterized by its low-frequency plateau value ( $S_{\text{o}}$ ) and corner frequency ( $f_{\text{c}}$ ) as  $S_{\text{o}}/[1 + (ff_{\text{c}})^2]$ , and high-frequency amplifier noise characterized by the coefficient  $S_2$  and the exponent  $\beta$  as  $S_2 \cdot f^\beta$  (20).

The  $f_{\text{c}}$  at 10 and 30 μM CDPC at the sequential time points were fit to smooth curves as described previously (TableCurve 2D), thereby filtering out small uncertainties in estimation of the individual  $f_{\text{c}}$  (20). The on ( $k_{\text{ob}}$ ) and off ( $k_{\text{bo}}$ ) rate coefficients for the channel transitions between open and blocked states were calculated from the slopes and intercepts of the filtered pairs of  $f_{\text{c}}$  at 10 and 30 μM CDPC, where  $2\pi f_{\text{c}} = k_{\text{ob}}B + k_{\text{bo}}$  and B is the blocker concentration. The blocker equilibrium constants ( $K_{\text{B}}$ ) were calculated as  $K_{\text{B}} = k_{\text{bo}}/k_{\text{ob}}$  (20).

**Single-channel currents.**  $i_{\text{Na}}$  were calculated at 10 μM CDPC with Eq. 1

$$i_{\text{Na}} = \frac{S_{\text{o}}}{P_{\text{gain}}} \left[ \frac{(2\pi f_{\text{c}})^2}{4I_{\text{Na}}k_{\text{ob}}B} \right] \quad (1)$$

The original equation (25) was modified to include a power gain correction ( $P_{\text{gain}}$ ; APPENDIX A). In contrast to frog skin, where the basolateral membrane capacitance ( $C_{\text{b}}$ ) is far greater in value than the apical membrane capacitance ( $C_{\text{a}}$ ) [due to the functional coupling of multiple cell layers that markedly increase basolateral membrane area and capacitance (3)], the basolateral membrane area in cell monolayers of A6 epithelia is far less in value in absolute terms and in terms relative to apical membrane area. Consequently, the fractional capacitance [ $C_{\text{b}}/(C_{\text{b}} + C_{\text{a}})$ ] is significantly less than unity in A6 epithelia compared with frog skin. The formal consequence for this area-related difference of capacitance is presented in APPENDIX A, leading to a correction for  $S_{\text{o}}$  by  $P_{\text{gain}}$  to account for attenuation of the Lorentzian power measured and the actual power originating within the apical membrane ENaCs. Accordingly, the current noise measured in short-circuit currents ( $I_{\text{sc}}^{\text{n}}$ ) underestimates the actual Na<sup>+</sup> current noise originating in the channels ( $I_{\text{Na}}^{\text{n}}$ ). If  $C_{\text{a}}$  and  $C_{\text{b}}$  at very low audio frequencies are 1.38 and 20 μF/cm<sup>2</sup>, respectively, as we have determined with impedance measurements of A6 epithelia grown on Transwell-Clear inserts (T. G. Păunescu and S. I. Helman, unpublished observations), then  $P_{\text{gain}}$  is 0.875. We have assumed constancy of  $P_{\text{gain}}$  in all calculations, recognizing that small differences among tissues will lead to relatively small uncertainties in determination of the single-channel currents.

**Open-channel densities.** Open-channel densities ( $N_o$ ) at 10  $\mu\text{M}$  CDPC ( $N_o^{10}$ ) were calculated as  $I_{\text{Na}}^{10}/i_{\text{Na}}^{10}$ , where the superscripts here and elsewhere indicate the blocker concentration.  $N_o$ , in the absence of blocker, was calculated as described previously (18, 20) with Eq. 2

$$N_o = N_o^{10} \left( 1 + \frac{P_o B^{10}}{K_B} \right) \quad (2)$$

**Channel open probabilities.** During control and experimental periods,  $P_o$  were calculated as described previously (20) with Eq. 3.  $N_o^{B_2/B_1}$  represents the quotient of open-channel densities ( $N_o^{B_2}/N_o^{B_1}$ ) determined at 10 ( $B_1$ ) and 30 ( $B_2$ )  $\mu\text{M}$  CDPC

$$P_o = \frac{1 - N_o^{B_2/B_1}}{B_2 N_o^{B_2/B_1} - B_1} K_B \quad (3)$$

Because  $N_o^B = I_{\text{Na}}^B/i_{\text{Na}}^B$ ,  $N_o^{B_2/B_1}$  can be equated with the quotient  $I_{\text{Na}}^{B_2/B_1}/i_{\text{Na}}^{B_2/B_1}$ , which represents the quotient of the fractional changes of macroscopic currents and the fractional changes of single-channel currents. Hence, open probability can be determined from the decreases of macroscopic rates of  $\text{Na}^+$  entry into the cells caused by increasing the CDPC concentration from 10 to 30  $\mu\text{M}$  and from the concurrent increases of single-channel currents that occur with hyperpolarization of apical membrane voltage. With small fractional changes of  $I_{\text{Na}}$ , relatively smaller fractional changes of apical membrane voltage are expected together with equally smaller changes of  $i_{\text{Na}}$ .  $i_{\text{Na}}^{30/10}$  were calculated with Eq. 7 (APPENDIX C).

**Functional channel densities.**  $N_T$  were calculated as the quotient  $N_o/P_o$ .  $N_T$  represents the total number of channels involved in apical membrane  $\text{Na}^+$  entry into the cells that fluctuate spontaneously between open and closed states of the channel. Channel densities are expressed in units of millions of channels per  $\text{cm}^2$  of planar area or per 100  $\mu\text{m}^2$ , approximating the planar area occupied by a single cell. It may be emphasized that channels or subunits of ENACs that reside within the apical membranes in nonfunctional or quiescent states would not be detected.

**Basolateral membrane resistance.** The basolateral membrane resistance ( $R_b$ ) was calculated at each time point with Eq. 5 (APPENDIX B).

**Statistical analysis.** Data are expressed as means  $\pm$  SE. Statistical analyses were performed with SigmaStat (Jandel Scientific) using paired or unpaired  $t$ -tests where appropriate. A  $P$  value  $<0.05$  was considered significant.

## RESULTS

**LY-294002 inhibits  $\text{Na}^+$  transport in unstimulated and aldosterone-prestimulated tissues.** Shown in Fig. 1 are typical strip-chart recordings of the  $I_{\text{sc}}$  response to 10 or 50  $\mu\text{M}$  LY-294002 added to the apical perfusion solution of either a control unstimulated tissue or a tissue that had been pretreated with aldosterone to stimulate its baseline rate of  $\text{Na}^+$  transport. After the tissues were short-circuited in chambers, the  $I_{\text{sc}}$  were allowed to stabilize for  $\sim 1.5$  h before onset of a 2-h control period that was followed by a 90-min experimental period, during which time the tissues were exposed to LY-294002. Subsequently, LY-294002 was removed from the apical solution for 2.5 h, and the experiments were terminated after complete inhibition of blocker-sensitive  $\text{Na}^+$  entry into the cells by 100  $\mu\text{M}$  amiloride.

Examination of these records indicated that inhibition of transport by LY-294002 was preceded within 1 min by a relatively small but readily apparent stimulation of  $I_{\text{sc}}$ , especially in those tissues treated with 50  $\mu\text{M}$  LY-294002 (Fig. 1C). Inhibition of  $I_{\text{sc}}$  proceeded relatively slowly with quasi-exponential time constants of 20.2, 22.1, and 13.4 min for the experiments shown in Figs. 1A, 1B, and 1C, respectively. It can be observed that the response to LY-294002 was more rapid in unstimulated tissues treated with the higher 50  $\mu\text{M}$  concentration of LY-294002 than with 10  $\mu\text{M}$  LY-294002 in unstimulated and aldosterone-prestimulated tissues. Inhibition of  $I_{\text{sc}}$  by LY-294002 was completely reversible with recovery of  $I_{\text{sc}}$  noticeably slower in those tissues treated with 50  $\mu\text{M}$  LY-294002.

Also indicated in Fig. 1 are the absolute changes of  $I_{\text{sc}}$  caused by increasing the CDPC concentration from 10 to 30  $\mu\text{M}$ . The measurements of  $I_{\text{sc}}^{10}$  and  $I_{\text{sc}}^{30}$  were obtained from data acquired digitally (8 points/s) at high resolution that permitted determination of the fractional changes of amiloride-sensitive currents,  $I_{\text{Na}}^{30/10}$ , within 60–90 s after the CDPC concentration was increased to 30  $\mu\text{M}$ . At these times, channels have redistributed between closed, open, and blocked states (20). PDS were acquired at 10  $\mu\text{M}$  CDPC just before elevation of CDPC to 30  $\mu\text{M}$ . PDS were also acquired at 30  $\mu\text{M}$  CDPC during the last 2 min of the 2-min, 40-s pulse durations, thereby yielding the  $f_c$  and  $S_o$  of the Lorentzians at 10 and 30  $\mu\text{M}$  CDPC.

**Stimulation precedes inhibition of  $I_{\text{sc}}$  caused by LY-294002.** Summarized in Fig. 2 are the initial increases of  $I_{\text{sc}}$  caused by LY-294002. The strip-chart digitized data (1 point/s) were normalized for the purpose of summarization to their zero time values at intervals of 25 s. LY-294002 (10  $\mu\text{M}$ ) caused relatively similar, small fractional increases of  $I_{\text{sc}}$  (mean of 4–5%) within 1–2 min, despite differences in baseline rates of  $\text{Na}^+$  transport in control and aldosterone-prestimulated tissues. With 50  $\mu\text{M}$  LY-294002,  $I_{\text{sc}}$  was increased absolutely and fractionally more so than with 10  $\mu\text{M}$  within 1–2 min (mean of 18%) before the  $I_{\text{sc}}$  began to return toward zero time values. Within 5 min,  $I_{\text{sc}}$  returned to zero time values and continued to decrease thereafter as indicated in Fig. 1.

Underlying the time-dependent changes of  $I_{\text{Na}}$  are differential time- and concentration-dependent changes of  $P_o$  and  $N_T$  (see *Time-dependent changes of  $P_o$*  and *Time-dependent changes of  $N_T$* ). The results of our analysis are summarized in Fig. 3 for unstimulated control and aldosterone-pretreated tissues challenged with 10  $\mu\text{M}$  LY-294002 and in Fig. 4 for unstimulated tissues challenged with 50  $\mu\text{M}$  LY-294002. The mean responses of the  $I_{\text{Na}}$  have been reported previously for tissues challenged with 10  $\mu\text{M}$  LY-294002 (5). The data presented in Fig. 4A indicate the average time course of inhibition of  $I_{\text{Na}}$  and its reversibility in unstimulated tissues challenged with 50  $\mu\text{M}$  LY-294002. Notably, the first time point of measurement after exposure to LY-294002 is at 5 min, so the initial stimulation of transport is not indicated in Figs. 3 and 4. During experimental periods, measurements of

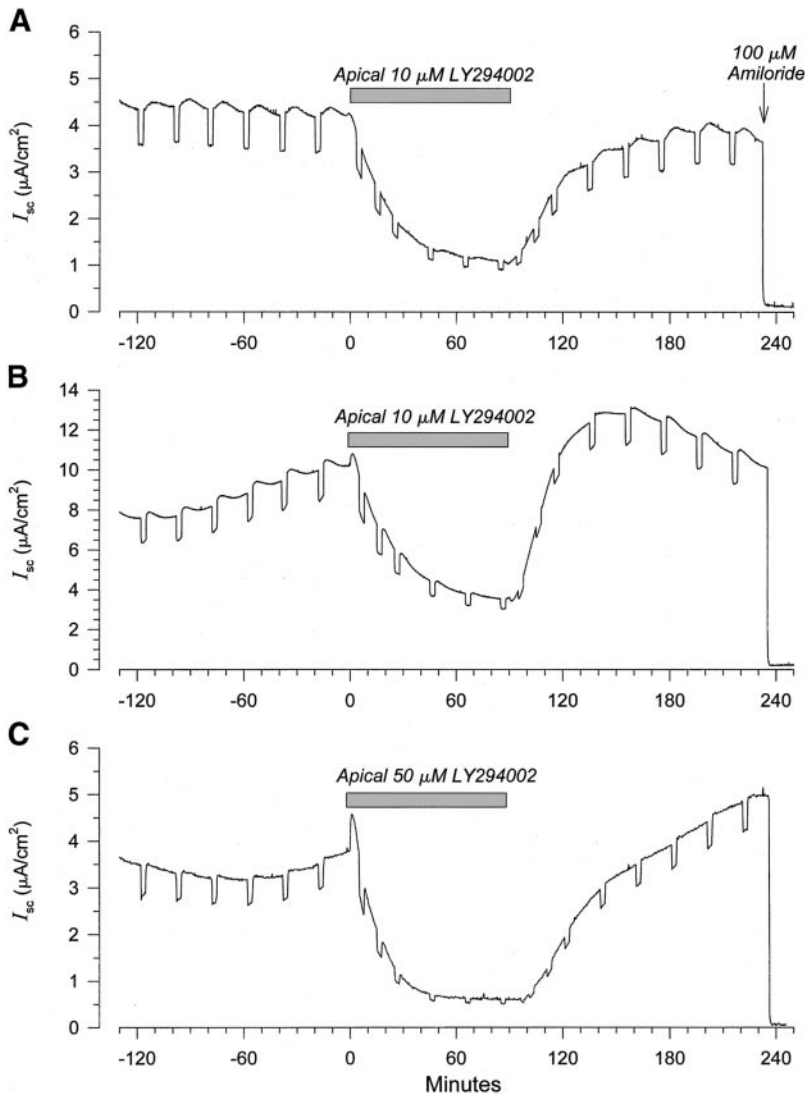


Fig. 1. Typical strip-chart records of the response of the short-circuit current ( $I_{sc}$ ) to addition of LY-294002 to the apical solution of an A6 epithelium. Unstimulated tissues were treated for 90 min with either 10 (A) or 50  $\mu\text{M}$  (C) LY-294002. Aldosterone-prestimulated tissues were treated with 10  $\mu\text{M}$  LY-294002 (B). After withdrawal of LY-294002 for 2.5 h, 100  $\mu\text{M}$  amiloride was added to the apical solution. The apical solution contained 10  $\mu\text{M}$  6-chloro-3,5-diamino-pyrazine-2-carboxamide (CDPC) except for the pulse periods when the CDPC concentration was increased to 30  $\mu\text{M}$ .

$i_{\text{Na}}$ ,  $P_o$ , and  $N_T$  were done at 5 min and thereafter at intervals of 10 min, whereas during control and recovery periods, measurements were made at intervals of 20 min. The zero time  $I_{\text{Na}}$  averaged  $4.00 \pm 0.14 \mu\text{A}/\text{cm}^2$  in unstimulated tissues ( $n = 5$ ) and was decreased by 10  $\mu\text{M}$  LY-294002 to  $1.33 \pm 0.25 \mu\text{A}/\text{cm}^2$ , or to  $33.1 \pm 5.8\%$  of zero time values, within 90 min. Despite aldosterone stimulation of  $I_{\text{Na}}$  to  $9.12 \pm 0.94 \mu\text{A}/\text{cm}^2$ , 10  $\mu\text{M}$  LY-294002 decreased  $I_{\text{Na}}$  to  $3.38 \pm 0.32 \mu\text{A}/\text{cm}^2$ , or fractionally to  $37.7 \pm 1.8\%$  of its elevated zero time values, and thus essentially to the same extent as was observed with unstimulated tissues. Unstimulated tissues challenged with 50  $\mu\text{M}$  LY-294002 responded more quickly, as indicated above, from zero time  $I_{\text{Na}}$  of  $3.42 \pm 0.24 \mu\text{A}/\text{cm}^2$ , reaching stable plateau values within 60 min and averaging  $0.79 \pm 0.24 \mu\text{A}/\text{cm}^2$  at 90 min ( $23.2 \pm 4.1\%$ ).

**Time-dependent changes of  $i_{\text{Na}}$ .** Our previous analysis had indicated that inhibition of transport could not be ascribed to changes of  $i_{\text{Na}}$  when control or aldosterone-prestimulated tissues were challenged with 10  $\mu\text{M}$  LY-294002 (5) or, as indicated in Fig. 4B, with 50  $\mu\text{M}$  LY-294002. At 5 min,  $i_{\text{Na}}$  was unchanged (5) or

essentially unchanged (Fig. 4B) from zero time values. At 15 min and thereafter, inhibition of transport was accompanied by relatively small increases of  $i_{\text{Na}}$  that were reversed on withdrawal of LY-294002 and return of  $I_{\text{Na}}$  toward and above zero time values. Such behavior of  $i_{\text{Na}}$  is expected and consistent with changes of fractional transcellular resistance [ $R_a/(R_a + R_b)$ ], where apical membrane resistance ( $R_a$ ) is increased (LY-294002 exposure) or decreased (LY-294002 withdrawn) relative to any change of basolateral membrane resistance ( $R_b$ ) (see *Changes of  $R_b$  caused by LY-294002*). Clearly, inhibition of  $I_{\text{Na}}$  could not be due to changes of  $i_{\text{Na}}$ , and so inhibition of transport at the apical membranes of the cells was due to time-dependent decrease of  $N_o$ .

Zero time single-channel currents averaged near 0.4 pA in all groups of experiments. With single-channel conductance ( $\gamma_{\text{Na}}$ ) equal to 5 pS, the absolute value of apical and basolateral membrane voltage would be 80 mV ( $i_{\text{Na}}/\gamma_{\text{Na}}$ ) at zero time and would have increased to  $\sim 90$  mV when  $i_{\text{Na}}$  was near 0.45 pA during tissue exposure to LY-294002.

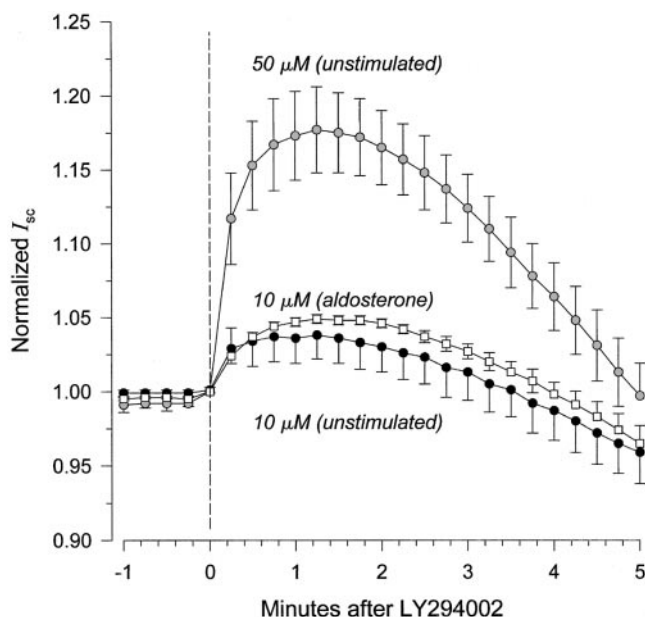


Fig. 2. Stimulation precedes inhibition of  $I_{sc}$  by LY-294002.  $I_{sc}$  were digitized at 1 point/s, and the data were summarized at intervals of 25 s. The first 5 min of data, normalized to zero time values, are shown following addition of LY-294002 to the apical solution. Values are means  $\pm$  SE. Unstimulated tissues were treated with either 10  $\mu\text{M}$  LY-294002 ( $n = 5$ ) or 50  $\mu\text{M}$  LY-294002 ( $n = 5$ ), and aldosterone-prestimulated tissues were treated with 10  $\mu\text{M}$  LY-294002 ( $n = 7$ ).

The  $f_c$  of the CDPC-induced Lorentzians and the blocker equilibrium constants ( $K_B$ ) for CDPC were similar in value to those reported previously for A6 epithelia (4, 14, 15, 20) and were unchanged by LY-294002 (data not shown).

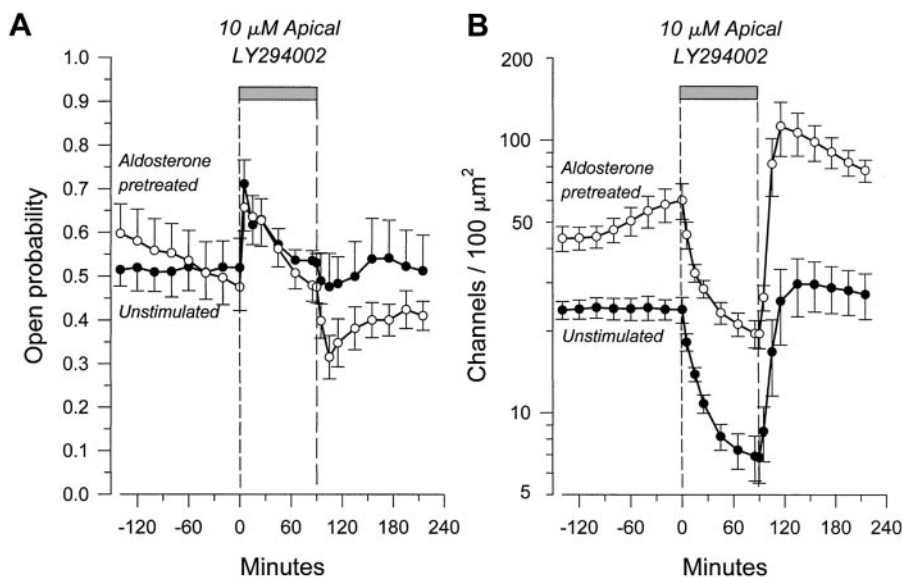
**Time-dependent changes of  $P_o$ .** LY-294002 caused changes of both  $P_o$  and  $N_T$ . However, the time courses and directions of change were entirely different. Figures 3A and 4C summarize the time-dependent changes of  $P_o$ . Within 5 min, the  $P_o$  were increased acutely by 10  $\mu\text{M}$  LY-294002 (Fig. 3A) and more so by

50  $\mu\text{M}$  LY-294002 (Fig. 4C). Zero time  $P_o$  averaged near 0.5 in unstimulated and aldosterone-prestimulated tissues challenged with 10  $\mu\text{M}$  LY-294002. The increases of  $P_o$  were essentially the same [to  $143 \pm 17\%$  (unstimulated) and to  $142 \pm 10\%$  of control (aldosterone)], despite differences in baseline rates of  $I_{Na}$  that averaged  $4.00 \pm 0.14$  and  $9.12 \pm 0.94 \mu\text{A}/\text{cm}^2$ , respectively, in unstimulated and aldosterone-prestimulated tissues (5). When tissues were challenged with 50  $\mu\text{M}$  LY-294002,  $P_o$  was increased from  $0.42 \pm 0.06$  to  $0.81 \pm 0.07$ , or to  $215 \pm 38.3\%$ , at 5 min (Fig. 4C). From maximum increases observed at 5 min, the  $P_o$  returned slowly over 90 min toward zero time values. On withdrawal of LY-294002,  $P_o$  was reversed toward or below zero time values and was particularly rapid in those tissues challenged with 50  $\mu\text{M}$  LY-294002.

It should be noted that  $P_o$  were calculated using the quotient  $I_{Na}^{30/10}/I_{Na}^{30/10} = N_o^{30/10}$ . Zero time values of  $I_{Na}^{30/10}$  averaged near 0.82 in all groups of tissues. Zero time values of  $I_{Na}^{30/10}$  averaged near 1.07 and remained essentially unchanged by LY-294002. Accordingly, the changes of  $P_o$  reflected the time-dependent changes of  $I_{Na}^{30/10}$  because the  $K_B$  were not changed by LY-294002, as indicated above.

**Time-dependent changes of  $N_T$ .** Compared with  $P_o$ , the directional change, time course, and concentration dependence of  $N_T$  on LY-294002 were completely different (Figs. 3B and 4D). At 10  $\mu\text{M}$  LY-294002 in unstimulated and aldosterone-prestimulated tissues (Fig. 3B),  $N_T$  decreased with quasi-exponential time constants of 16.9 and 19.6 min, and from zero time values of  $24.0 \pm 2.6$  and  $60.3 \pm 9.0$  channels/ $100 \mu\text{m}^2$ , respectively. Parenthetically, aldosterone stimulation of transport in these groups of experiments is due solely to increase of  $N_T$  and is the same as reported previously (20). At 90 min,  $N_T$  was decreased to  $6.9 \pm 1.3$  (unstimulated) and  $19.5 \pm 2.3$  (aldosterone) channels/ $100 \mu\text{m}^2$ , or to  $28.4 \pm 3.7\%$  and  $34.5 \pm 3.1\%$  of zero time values, respectively, irrespective of the 2.5-fold

Fig. 3. Summary of the changes of channel open probability ( $P_o$ ) (A) and functional channel density ( $N_T$ ) (B) caused by 10  $\mu\text{M}$  LY-294002 in unstimulated ( $n = 5$ ) and aldosterone-prestimulated ( $n = 7$ ) tissues. Values are means  $\pm$  SE. Tissues were exposed to LY-294002 for 90 min and allowed to recover after withdrawal of LY-294002 from the apical solution. Comparison of the time-dependent changes of  $P_o$  and  $N_T$  with those of the open-channel density ( $N_o = P_o N_T$ ) reported previously (5) underscores the importance of resolving time-dependent changes of  $N_o$  into the individual changes of  $P_o$  and  $N_T$ . Notably, underlying the apparently simple time-dependent changes of  $N_o$  are more complex changes of  $P_o$  and  $N_T$ . Compare these data, obtained with 10  $\mu\text{M}$  LY-294002, with the data obtained with 50  $\mu\text{M}$  LY-294002 presented in Fig. 4.



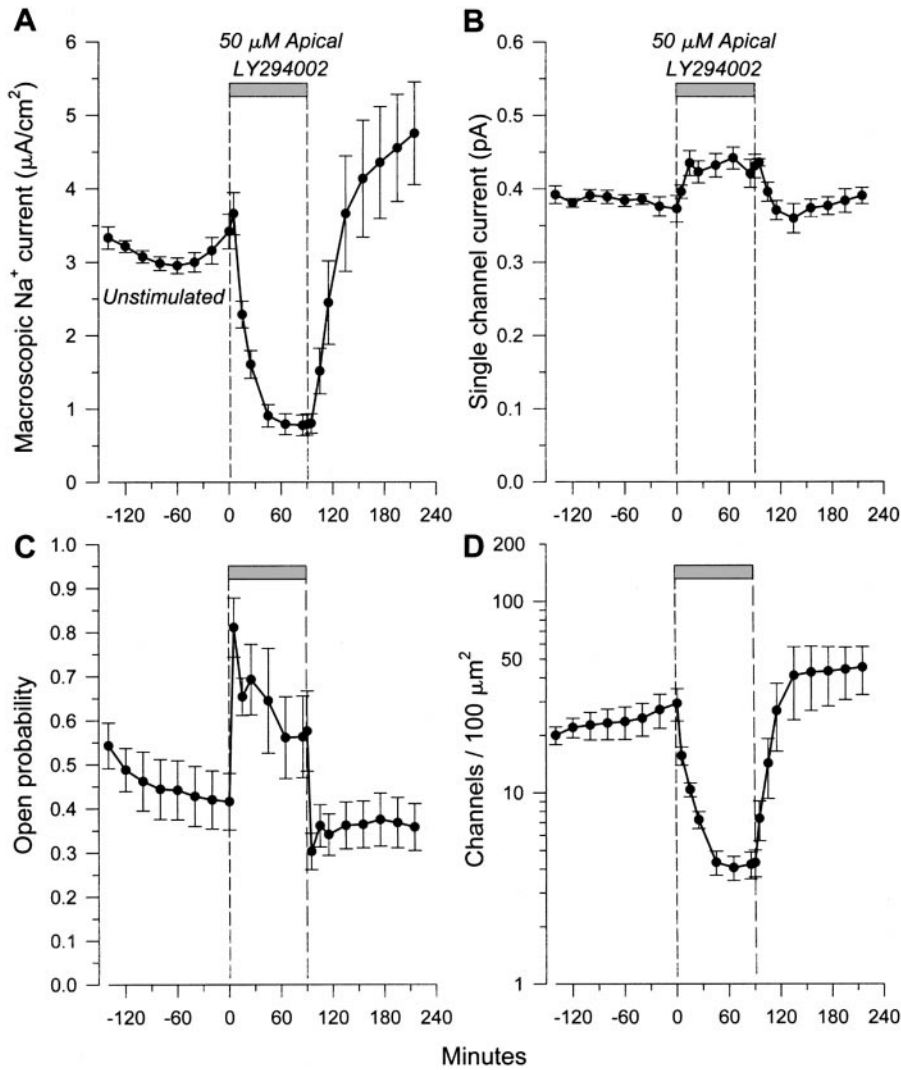


Fig. 4. Summary of the changes of macroscopic  $\text{Na}^+$  current ( $I_{\text{Na}}$ ) (A), single-channel current ( $i_{\text{Na}}$ ) (B),  $P_o$  (C), and  $N_T$  (D) caused by 50  $\mu\text{M}$  LY-294002 in unstimulated tissues ( $n = 5$ ). Values are means  $\pm$  SE. Compare these data with the data presented in Fig. 3.

difference of zero time values. The limiting values of  $N_T$  derived from the exponential fits of data indicated that at infinite time,  $N_T$  would have stabilized at 28.1% (unstimulated) and 30.7% (aldosterone) of zero time values in tissues treated with 10  $\mu\text{M}$  LY-294002.

Compared with tissues treated with 10  $\mu\text{M}$  LY-294002, the  $N_T$  of tissues treated with 50  $\mu\text{M}$  LY-294002 decreased more rapidly with a time constant of 10.9 min, reaching stable values within  $\sim 60$  min (Fig. 4D). From zero time values that averaged  $29.4 \pm 5.6$  channels/ $100 \mu\text{m}^2$ ,  $N_T$  was decreased to  $4.3 \pm 0.7$  channels/ $100 \mu\text{m}^2$  at 90 min, or to  $15.3 \pm 1.7\%$  of zero time values.

*LY-294002 does not act from the basolateral surface of the tissues.* LY-294002 presented to the tissues at their basolateral surface was, surprisingly, completely without effect on  $\text{Na}^+$  transport (Fig. 5). The typical patterns of inhibition of  $I_{\text{Na}}$  elicited by apically applied LY-294002 at the same concentration (10  $\mu\text{M}$ ) were completely absent, as were the changes of  $i_{\text{Na}}$ ,  $P_o$ , and  $N_T$ . To the extent that apical and basolateral membrane permeabilities to LY-294002 are the same (per unit area) and to the extent that basolateral membrane

surface area is far greater than apical membrane surface area, the actual concentration of intracellular LY-294002 should be far greater when LY-294002 is presented to the tissues from the basolateral solution. Consequently, the absence of detectable changes of transport is most surprising if it is assumed that the LY-294002 inhibitable PI 3-kinase is accessible equally well from the extracellular fluids bathing the apical and basolateral surfaces of the cells. Clearly, a simple cytoplasmic site(s) of action is precluded among schemes that may ultimately explain how LY-294002 causes both increase of  $P_o$  and decrease of  $N_T$  with entirely different time courses, but only when cells are presented with LY-294002 from the apical face of the cells.

*Changes of  $R_b$  caused by LY-294002.* Although not a major aim of these studies, it was of interest to know if apical LY-294002 caused changes of the basolateral membrane resistance of the cells. Calculations were carried out with Eq. 5 (APPENDIX B) and the results summarized as indicated in Fig. 6. Zero time  $R_b$  of unstimulated tissues averaged  $9,028 \pm 783 \Omega \cdot \text{cm}^2$  ( $n = 15$ ), whereas those of aldosterone-prestimulated

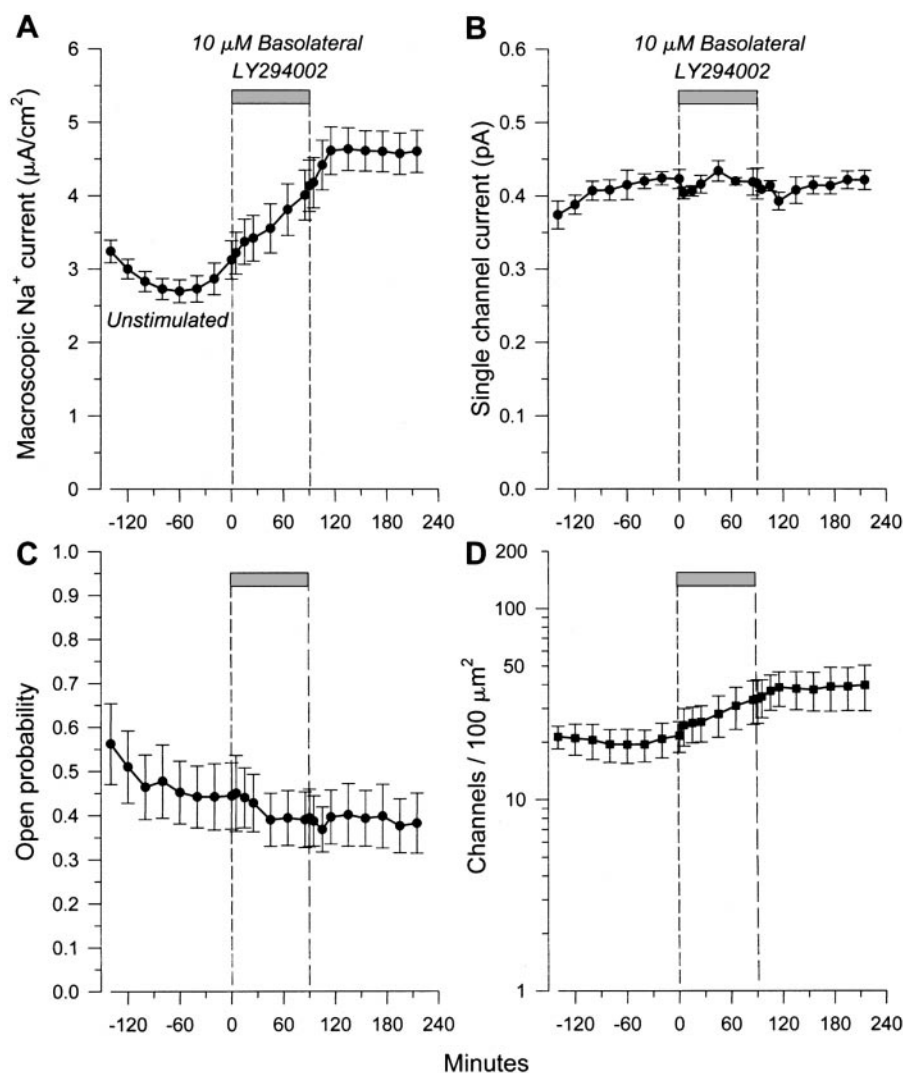


Fig. 5. Absence of change of  $I_{\text{Na}}$  (A),  $i_{\text{Na}}$  (B),  $P_o$  (C), and  $N_T$  (D) when tissues ( $n = 5$ ) are presented with  $10 \mu\text{M}$  LY-294002 applied at the basolateral membrane surface. Values are means  $\pm$  SE. Compare these data with the data presented in Figs. 3 and 4.

tissues averaged  $3,864 \pm 879 \Omega \cdot \text{cm}^2$  ( $n = 7$ ). Thus steroid stimulation of transport by aldosterone was mediated not only by increases of apical membrane  $N_T$  but also by increases of basolateral membrane conductance, due most likely to activation of a basolateral membrane  $\text{K}^+$  conductance as suggested originally by Schultz (35). Whereas stimulation of transport by aldosterone was accompanied by decrease of  $R_b$ , inhibition of transport by LY-294002 was accompanied by a reversible increase of  $R_b$  as indicated in Fig. 6A. When normalized to zero time values as shown in Fig. 6B, the fractional increases of  $R_b$  were essentially the same in unstimulated and aldosterone-prestimulated tissues at 10 and 50  $\mu\text{M}$  LY-294002. At 90 min,  $R_b$  was increased about two- to threefold above zero time values. Notably, however, LY-294002-related increases of  $R_b$  were delayed by at least 15 min from onset of the increases of  $P_o$  reported above and the decreases of  $N_T$  that were observed during this same time period. In this regard, it also remains curious that LY-294002 applied to the basolateral membrane is without effect on  $R_b$ , suggesting that changes of  $R_b$  do not occur by direct interaction of LY-294002 with the basolateral membrane of the

cells or by access to the cytosol from the basolateral surface of the cells.

## DISCUSSION

We have examined the role of an LY-294002-sensitive PI 3-kinase in modulating basal (unstimulated) and aldosterone-prestimulated  $\text{Na}^+$  transport in cell-cultured A6 epithelia derived from the renal distal tubule of *Xenopus laevis*. A noninvasive pulse method of weak blocker-induced noise analysis was used to determine whether inhibition of transport in response to LY-294002 was due to changes of  $i_{\text{Na}}$ ,  $N_T$ , and/or  $P_o$  that together determine the overall effect of the inhibitor on  $\text{Na}^+$  transport.

Our analysis has revealed that apical exposure of A6 epithelia to LY-294002 causes, after a relatively small initial stimulation, a marked and completely reversible inhibition of both basal and aldosterone-prestimulated  $\text{Na}^+$  transport due to slow time-dependent decreases of functional ENaC densities within the apical membranes of the cells. The initial stimulation of transport was due to considerably more rapid but quantitatively

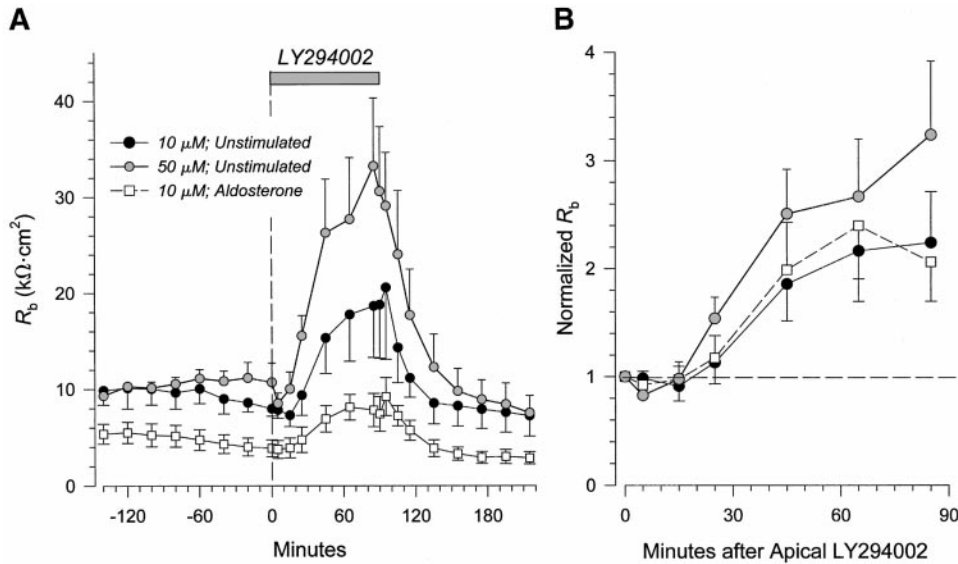


Fig. 6. Apical LY-294002 causes a delayed and reversible increase of basolateral membrane resistance ( $R_b$ ) (A). From the zero time normalized values of  $R_b$  shown in (B), the delay time for increase of  $R_b$  is estimated to be at least 15 min. Values are means  $\pm$  SE. Note also that the fractional increases of  $R_b$  are essentially the same in unstimulated and aldosterone-prestimulated tissues treated with 10  $\mu\text{M}$  LY-294002 and in unstimulated tissues treated with 50  $\mu\text{M}$  LY-294002.

smaller fractional increases of ENaC  $P_o$ . LY-294002 applied apically not only increased apical membrane resistance (decrease of ENaC  $N_T$ ) but also caused, after a substantial delay, a reversible increase of basolateral membrane resistance. Similar qualitative changes were seen at 10 and 50  $\mu\text{M}$  LY-294002. However, significant differences became apparent not only in the time course of change of the  $P_o$  and  $N_T$  but also in the sensitivity of the  $P_o$  and  $N_T$  to these concentrations of LY-294002.

The difference in sensitivity of the  $P_o$  and the  $N_T$  to LY-294002 is emphasized in Fig. 7. Near-maximal increases of  $P_o$  were measured at 5 min. The response at 5 min expressed in absolute terms (Figs. 3 and 4) or normalized to zero time values (Fig. 7) indicated clearly that  $P_o$  was concentration dependent in the range of 10–50  $\mu\text{M}$  LY-294002. With  $P_o$  averaging in the range of 0.4–0.5, the maximal increases of  $P_o$  would not exceed a normalized increase of  $\sim$ 2- to 2.5-fold, so the increases of  $P_o$  at 50  $\mu\text{M}$  LY-294002 are close to the maximum that can be elicited by LY-294002. Accordingly, regardless of mechanism, a half-maximal concentration of LY-294002 in the range of  $\sim$ 15–20  $\mu\text{M}$  LY-294002 would be required to cause a 50% increase of  $P_o$ .

Maximal or near-maximal decreases of  $N_T$  could be elicited by LY-294002 within 60 min at 50  $\mu\text{M}$  and within 90 min at 10  $\mu\text{M}$  (Figs. 3 and 4). Examination of the normalized decreases of  $N_T$  (Fig. 7) indicated that  $N_T$  was most sensitive to LY-294002 at concentrations  $<10$   $\mu\text{M}$ . The dependency of  $N_T$  on LY-294002 could as a first approximation be reasonably characterized by an  $\text{IC}_{50}$  in the range of 1–2  $\mu\text{M}$  LY-294002, which would be remarkably close to the  $\text{IC}_{50}$  of 1.4  $\mu\text{M}$  of the LY-294002 inhibitable PI 3-kinase reported by Vlahos et al. (40).

It is thus interesting to note that the response of  $N_T$  to LY-294002 is most likely attributable to an LY-294002 inhibitable PI 3-kinase. This PI 3-kinase is involved directly at least in one of the steps or pro-

cesses mediating regulation of apical membrane ENaC densities. Stimulation of transport by insulin and aldosterone is mediated by increases of  $N_T$  (4, 20), and LY-294002 inhibits both the insulin- and aldosterone-mediated increases of transport (5, 31). It remains to be determined whether LY-294002 inhibits hormone-stimulated transport by preventing increases of  $N_T$ . If LY-294002 causes substantial increases of  $P_o$  as reported here, then the LY-294002-mediated prevention of a threefold or greater stimulation of transport by aldosterone and/or insulin must be due, on quantita-

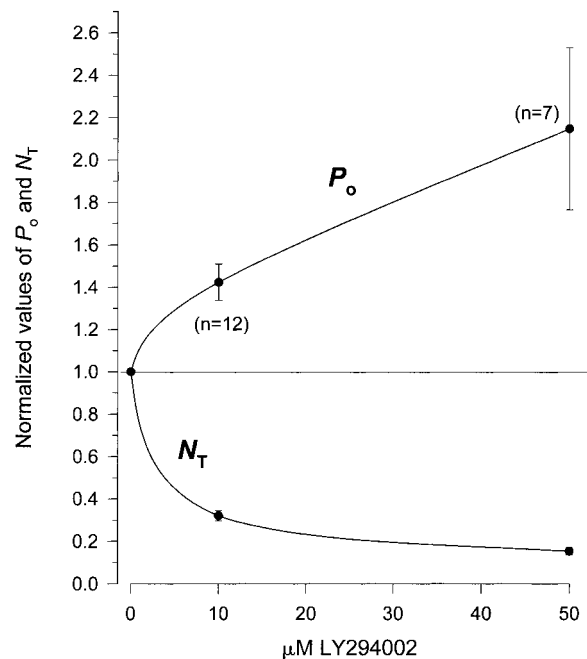


Fig. 7. Dependence of  $P_o$  and  $N_T$  on the concentration of LY-294002. Data are plotted as zero time normalized values at 5 min ( $P_o$ ) and at 90 min ( $N_T$ ). Values are means  $\pm$  SE. Data points at 10  $\mu\text{M}$  LY-294002 are combined from unstimulated and aldosterone-prestimulated tissues. Solid lines are spline fits to the data points.

tive grounds, to loss of hormone-mediated increases of  $N_T$ .

It may be useful to note that we are not aware, at least from our own studies, of how the  $P_o$  of ENaC is regulated in intact epithelial cells. It is thus, at this time, impossible to know how and why LY-294002 increases  $P_o$  in reversible fashion. The concentrations of LY-294002 required to increase  $P_o$  are substantially greater than those required to decrease  $N_T$ . Whether this action of LY-294002 on  $P_o$  is a nonspecific effect or an effect mediated by yet another PI 3-kinase or a PI 3-kinase with a different  $IC_{50}$  remains to be determined, among other possibilities. Notably, whatever the mechanism, it was readily apparent that the effect of LY-294002 on  $P_o$  occurred rapidly (minutes) and reversibly.

Understanding the complex interactions that regulate the channel kinetics of ENaCs will require a detailed analysis of all the potential effectors in the regulatory pathway(s). Activation of PI 3-kinase is an early step in the phosphoinositide pathway, which typically includes downstream kinase cascades. Which of the effector pathways forms the physical link to ENaC via PI 3-kinase activation is unknown.

Interestingly, one of the kinases that is activated downstream of PI 3-kinase, the serum glucocorticoid-induced kinase (sgk), has recently been shown to be an aldosterone-induced protein (10, 29). Coexpression of sgk and ENaC in oocytes leads to increased Na<sup>+</sup> flux, suggesting that sgk can regulate channel activity. However, we have previously shown that aldosterone treatment has a direct effect on phosphatidylinositol phosphorylation, indicating the existence of another aldosterone-induced protein at or before the PI 3-kinase step, which is well before the sgk protein (5). Thus multiple components of the phosphoinositide pathway may be induced by aldosterone, whereas a constitutive level of activation of the pathway appears to be necessary for maintaining basal transport. The task of identifying each of the proteins, their functions as well as the number of steps in the complete pathway(s), remains a challenge for future investigations.

*Sided action of LY-294002.* Our results with regard to the ineffectiveness of LY-294002 when applied to the basolateral surface were completely unexpected. LY-294002 acts exclusively from the apical surface of the epithelium, with no significant effects on  $I_{Na}$ ,  $N_T$ ,  $P_o$ , and  $R_b$  when presented at the same concentration to the basolateral surface of the tissues. To our knowledge, this is a novel finding because this inhibitor is known to exhibit equal efficacy in whole cell assays using both adherent and suspended cells and in *in vitro* enzyme assays, suggesting that it is membrane permeable (40) (C. J. Vlahos, personal communication). The striking absence of response to basolateral LY-294002 is clearly not consistent with the action of a membrane-permeable inhibitor blocking the activity of a cytosolic enzyme.

Our finding suggests that the current view of PI 3-kinase as a cytosolic enzyme (at least of the LY-

294002 inhibitable PI 3-kinase) that is translocated to the membrane on activation may be too simplistic. In many experiments, "cytosolic" simply means that the enzyme is found in the soluble fraction during subcellular fractionation procedures after cellular disruption. Likewise, "membrane bound" simply means associated with a membrane fraction during the fractionation procedure. Neither of these terms allows one to assess exactly where in the cell the enzyme may be found.

It is difficult to imagine that a single event such as the binding of the catalytic subunit of PI 3-kinase to a phosphorylated intermediate (e.g., insulin receptor substrate) will cause the enzyme to migrate through the cytoplasm of the cell to a very specific area of the cell membrane. Rather, it is easier to imagine that complexes of intermediates may reside in close proximity to the final effectors. To our knowledge, there have been no detailed studies attempting to localize PI 3-kinase within the cytosolic or membrane subcompartments. This task will be complicated by the number of isoforms of PI 3-kinase that may be localized in various compartments, respond to different stimuli, and have different substrates. Our results suggest that the PI 3-kinases that are responsible for basal as well as hormone-stimulated Na<sup>+</sup> transport are localized and compartmentalized in such a way that only apically applied LY-294002 is effective. Further investigations are required to resolve unequivocally whether LY-294002 can traverse the plasma membrane and to determine precisely the localization of the specific PI 3-kinase that is involved in the modulation of membrane ion transport.

Our results do not prove, but are consistent with the idea, that LY-294002 prevents insertion and/or stimulates withdrawal of ENaCs from the apical plasma membrane of A6 cells. A similar effect was demonstrated for A-type potassium channels in hippocampal pyramidal neurons (41). In these cells, LY-294002 and wortmannin inhibition of PI 3-kinase was shown to cause decreases of membrane area and three different types of K<sup>+</sup> currents. Both wortmannin and LY-294002 induced a decrease of A-type K<sup>+</sup> channel density within the plasma membrane.

There are, however, a large number of studies that describe how PI 3-kinase plays a crucial role in endocytotic and/or exocytotic phenomena (2, 6, 8, 9, 16, 23, 24, 33, 38) [see also reviews by Shepherd et al. (37) and De Camilli et al. (12) and references therein]. Our own data do not rule out the possibility that PI 3-kinase may be involved in withdrawal of channels from the apical membrane because, on balance, the steady-state apical membrane density of functional ENaCs will be determined by the rates of insertion and withdrawal. Analogously, PI 3-kinase inhibition was shown to induce a decrease in the endosomal recycling of intracellular NHE3 isoforms of the Na<sup>+</sup>/H<sup>+</sup> exchanger to the cell membrane in AP-1 Chinese hamster ovary cells (23). On the weight of the available evidence cited above, our bias favors the view that PI 3-kinase is involved in shuttling of channels to and/or from the

apical membrane of the cells. However, we cannot rule out the possibility that PI 3-kinase is involved in recruiting channels and/or subunits from quiescent or nonfunctional states that are resident within the apical plasma membranes of the cells.

Thus, in summary, it will be most interesting to resolve where and how LY-294002 inhibitable PI 3-kinase is involved in regulation of basal ENaC channel densities and to learn at what step or steps PI 3-kinase is required for the hormonal response to insulin and aldosterone in regulation of transepithelial absorption of sodium. Our findings suggest that LY-294002 inhibits a novel member of the PI 3-kinase family involved in regulation of epithelial sodium channels.

## APPENDIX A

### Correction of the Lorentzian $S_o$ for Power Gain Loss

Shown in Fig. 8 are the usual direct current (DC) and alternating current (AC) electrical equivalent circuits of short-circuited epithelia with apical ( $R_a$  and  $C_a$ ) and basolateral ( $R_b$  and  $C_b$ ) membrane slope resistances and capacitances.  $E_b$  is the Thévenin electromotive force (EMF) of the basolateral membrane with values that exceed the potassium equilibrium potential difference due to the contribution of the current generated by the Na<sup>+</sup>-K<sup>+</sup>-ATPase pump current flowing through  $R_b$  (17, 21). Because the electrical operating point of apical membrane ENaCs is far removed from equilibrium, the Thévenin  $E_a$  is at or very near zero, so the apical

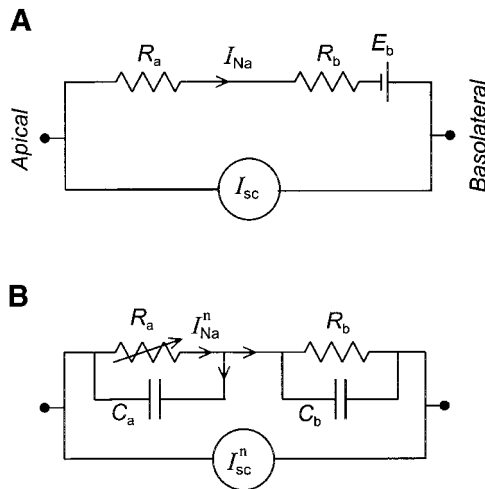


Fig. 8. Electrical equivalent circuits of a short-circuited A6 epithelium with an apical plasma membrane containing epithelial Na<sup>+</sup> channels (ENaCs). The apical membrane of the direct current (DC) equivalent circuit (A) is modeled by its slope resistance ( $R_a$ ) at physiological voltages far removed from electrochemical equilibrium. The basolateral membrane is modeled by its Thévenin electromotive force (EMF;  $E_b$ ) and slope resistance ( $R_b$ ). The DC apical membrane current carried into the cell is  $I_{Na}$ , where  $I_{Na} = I_{sc} = E_b / (R_a + R_b)$ . The alternating current (AC) equivalent circuit (B) additionally contains apical ( $C_a$ ) and basolateral ( $C_b$ ) membrane capacitances (EMF's behave as short-circuits in AC circuits). Conductance fluctuations of the channels give rise to sodium current noise ( $I_{Na}^n$ ).  $C_a$  and the parallel combination of  $R_b$  and  $C_b$  act as a frequency-dependent current divider. A fraction of  $I_{Na}^n$  is shunted back to the apical solution, whereas the current flowing through the basolateral membrane appears as current noise in the short-circuit ( $I_{sc}^n$ ). Hence,  $I_{sc}^n < I_{Na}^n$ .

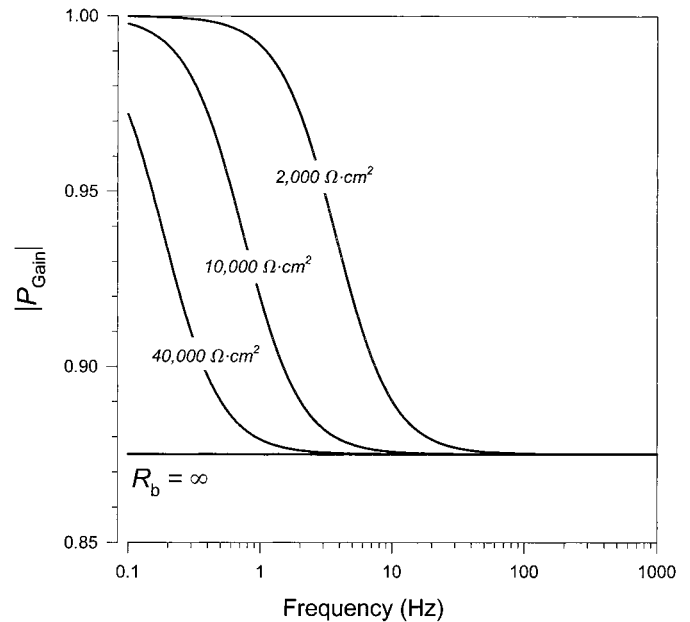


Fig. 9. The absolute value of power gain ( $|P_{gain}|$ , see text) was calculated at frequencies between 0.1 and 1,000 Hz for  $R_b$  between 2,000  $\Omega \cdot \text{cm}^2$  and infinity ( $C_a = 1.38 \mu\text{F}/\text{cm}^2$ ;  $C_b = 20 \mu\text{F}/\text{cm}^2$ ). The limiting value at the higher frequencies is 0.875.

membrane behaves electrically as a resistor paralleled by its capacitance.

In the presence of a Na<sup>+</sup> channel blocker, the conductance fluctuations of ENaCs between open and blocked states give rise to ac current noise ( $I_{Na}^n$ ). With  $C_a$ , the basolateral membrane conductance ( $G_b$ ), and  $C_b$  acting as a current divider, the short-circuit AC noise ( $I_{sc}^n$ ) is less than  $I_{Na}^n$ . Defining the noise current gain ( $I_{gain}$ ) as

$$I_{gain} = \frac{I_{sc}^n}{I_{Na}^n} = \frac{G_b + j\omega C_b}{G_b + j\omega(C_a + C_b)} \quad (4)$$

and the power gain as  $P_{gain} = (I_{gain})^2$ , the absolute value of  $P_{gain}$  ( $|P_{gain}|$ ) can be calculated as indicated in Fig. 9. For the purpose of calculation relevant to the study of A6 epithelia grown on Transwell-Clear substrates, we have calculated the power gain using DC capacitances of 1.38 and 20  $\mu\text{F}/\text{cm}^2$  for  $C_a$  and  $C_b$ , respectively (T. G. Păunescu and S. I. Helman, unpublished observations).  $|P_{gain}|$  approaches a limiting value of 0.875 with increasing frequency in the range of ~0.1–10 Hz that encompasses the range of  $R_b$  encountered in our experiments (see RESULTS). Consequently, spectral density power levels arising from Na<sup>+</sup> channel Lorentzian current noise will be underestimated by ~12.5% at frequencies greater than ~10 Hz. For  $R_b$  between 2,000 and 40,000  $\Omega \cdot \text{cm}^2$ , our calculations indicate that the half-power point frequencies for transition between upper and lower bounds of  $P_{gain}$  are 3.74 and 0.19 Hz, respectively.

It may be noted in particular for CDPC-induced noise that the corner frequencies of the Lorentzians range upward from ~40 Hz, so current noise power levels at these and higher frequencies are attenuated by the limiting value of  $|P_{gain}|$ , as indicated above. At much lower frequencies, ~10 Hz and less, and in the range of the  $1/f$  noise that far exceeds in value the power levels of the plateau values of the Lorentzians, Lorentzian noise contributes negligibly to the total power measured. Accordingly, the  $S_o$  values of the Lorentzians measured were corrected as indicated in Eq. 1 for attenuation of

current noise attributable to recirculation of Na<sup>+</sup> current noise through the apical membrane capacitance.

## APPENDIX B

### Calculation of $R_b$

While tissues are short-circuited, the absolute values of apical and basolateral membrane voltages ( $V_a$  and  $V_b$ , respectively) must be identical. If single-channel conductance of ENaCs ( $\gamma_{Na}$ ) averages near 5 pS (100 mM apical Na<sup>+</sup> concentration) (25), then membrane voltages can be estimated at every time point of our studies from the quotient  $i_{Na}^{10}/\gamma_{Na}$ . For typical single-channel currents near 0.4 pA,  $V_a = V_b = 80$  mV, which is in the range expected for a short-circuited tight epithelial cell with transepithelial transport of Na<sup>+</sup> rate limited by the apical membrane ENaC resistance of the cell. Because  $V_b = E_b - I_{sc}R_b$ ,  $R_b$  can be calculated as

$$R_b = \frac{E_b - (i_{Na}^{10}/\gamma_{Na})}{I_{sc}^{10}} \quad (5)$$

As in frog skin and other tight Na<sup>+</sup>-transporting epithelia (17, 21, 22, 26), the  $E_b$  of A6 epithelia has been determined to average near 110 mV both in untreated and aldosterone-prestimulated epithelia and over at least a threefold difference in rates of Na<sup>+</sup> transport (19). Although  $E_b$  is not strictly a constant, and to the extent that it can vary among tissues between ~100 and 120 mV, there is an ~20% uncertainty in obtaining absolute values of  $R_b$  if  $E_b$  is assumed to be constant, as we have done in our calculations. To the extent that we are interested in measuring changes of  $R_b$ , changes of  $R_b$  greater than ~20% were considered significant.

## APPENDIX C

### Blocker Concentration-Related Changes of Single-Channel Currents

Inhibition of apical membrane Na<sup>+</sup> entry by amiloride and other ENaC blockers causes hyperpolarization of apical membrane voltage as expected according to the DC electrical equivalent circuit shown in Fig. 8A. Changes in voltage are determined by the changes of fractional transcellular resistance  $fR_a = R_a/(R_a + R_b)$ , where  $V_a = fR_a E_b$  with reference to a grounded apical solution (19). Because changes of  $V_a$  are directly proportional to changes of  $i_{Na}$

$$\frac{\Delta V_a}{V_a} = \frac{-\Delta I_{sc} R_b}{i_{Na}^{10}/\gamma_{Na}} = \frac{\Delta i_{Na}}{i_{Na}^{10}} \quad (6)$$

For the case in which CDPC concentration is increased from 10 to 30  $\mu$ M with single-channel currents  $i_{Na}^{10}$  and  $i_{Na}^{30}$ , respectively, the ratio  $i_{Na}^{30}/i_{Na}^{10}$ , to be referred to as  $i_{Na}^{30/10}$ , can be calculated with Eq. 7. Because  $(i_{Na}^{30/10} - 1) = \Delta i_{Na}/i_{Na}^{10}$ , it can be shown that

$$i_{Na}^{30/10} = 1 + (1 - I_{sc}^{30/10}) \left[ \frac{E_b}{i_{Na}^{10}/\gamma_{Na}} - 1 \right] \quad (7)$$

where  $I_{sc}^{30/10}$  represents the ratio of short-circuit currents at 30 and 10  $\mu$ M CDPC. Here, as above, our goal is to measure changes of  $P_o$ . The assumption of constancy of  $E_b$  among tissues would result in small absolute errors (~5%) of  $i_{Na}^{30/10}$ , and hence  $P_o$ , but would not alter the outcome of calculations where the fractional changes of  $I_{Na}^{30/10}$  are

considerably larger than those of  $i_{Na}^{30/10}$ , as is the case for our experiments.

We gratefully acknowledge the meticulous work of A. L. Helman in the growth and preparation of the A6 epithelia and in the care of our tissue culture facility.

This work was supported by National Institute of Diabetes and Digestive and Kidney Diseases Grant DK-30824 to S. I. Helman and with American Heart Association (Indiana Affiliate) support to B. L. Blazer-Yost.

This work was carried out while T. G. Păunescu was a doctoral candidate in the Center for Biophysics and Computational Biology at the University of Illinois at Urbana-Champaign.

Present address of T. G. Păunescu: Dept. of Molecular and Integrative Physiology, 524 Burrill Hall, University of Illinois at Urbana-Champaign, Urbana, IL 61801.

## REFERENCES

1. Abramcheck FJ, Van Driessche W, and Helman SI. Auto-regulation of apical membrane Na<sup>+</sup> permeability of tight epithelia. Noise analysis with amiloride and CGS 4270. *J Gen Physiol* 85: 555–582, 1985.
2. Araki N, Johnson MT, and Swanson JA. A role for phosphoinositide 3-kinase in the completion of macropinocytosis and phagocytosis by macrophages. *J Cell Biol* 135: 1249–1260, 1996.
3. Awayda MS, Van Driessche W, and Helman SI. Frequency-dependent capacitance of the apical membrane of frog skin: dielectric relaxation processes. *Biophys J* 76: 219–232, 1999.
4. Blazer-Yost BL, Liu X, and Helman SI. Hormonal regulation of ENaCs: insulin and aldosterone. *Am J Physiol Cell Physiol* 274: C1373–C1379, 1998.
5. Blazer-Yost BL, Păunescu TG, Helman SI, Lee KD, and Vlahos CJ. Phosphatidylinositol 3-kinase is required for aldosterone regulated sodium reabsorption. *Am J Physiol Cell Physiol* 277: C531–C536, 1999.
6. Brunskill NJ, Stuart J, Tobin AB, Walls J, and Nahorski S. Receptor-mediated endocytosis of albumin by kidney proximal tubule cells is regulated by phosphatidylinositide 3-kinase. *J Clin Invest* 101: 2140–2150, 1998.
7. Carpenter CL and Cantley LC. Phosphoinositide kinases. *Biochemistry* 29: 11147–11156, 1990.
8. Chasserot-Golaz S, Hubert P, Thiersé D, Dirrig S, Vlahos CJ, Aunis D, and Bader MF. Possible involvement of phosphatidylinositol 3-kinase in regulated exocytosis: studies in chromaffin cells with inhibitor LY294002. *J Neurochem* 70: 2347–2356, 1998.
9. Cheatham B, Vlahos CJ, Cheatham L, Wang L, Blenis J, and Kahn CR. Phosphatidylinositol 3-kinase activation is required for insulin stimulation of pp70 S6 kinase, DNA synthesis, and glucose transporter translocation. *Mol Cell Biol* 14: 4902–4911, 1994.
10. Chen SY, Bhargava A, Mastroberardino L, Meijer OC, Wang J, Buse P, Firestone GL, Verrey F, and Pearce D. Epithelial sodium channel regulated by aldosterone-induced protein sgk. *Proc Natl Acad Sci USA* 96: 2514–2519, 1999.
11. Cross MJ, Stewart A, Hodgkin MN, Kerr DJ, and Wakelam MJ. Wortmannin and demethoxyviridin inhibit insulin stimulated phospholipase A2 activity in Swiss 3T3 cells. *J Biol Chem* 267: 2157–2163, 1992.
12. De Camilli P, Emr SD, McPherson PS, and Novick P. Phosphoinositides as regulators in membrane traffic. *Science* 27: 1533–1539, 1996.
13. Egawa K, Sharma PM, Nakashima N, Huang Y, Huver E, Boss GR, and Olefsky JM. Membrane-targeted phosphatidylinositol 3-kinase mimics insulin actions and induces a state of cellular insulin resistance. *J Biol Chem* 274: 14306–14314, 1999.
14. Els WJ and Helman SI. Dual role of prostaglandins (PGE<sub>2</sub>) in regulation of channel density and open probability of epithelial Na<sup>+</sup> channels in frog skin (*R. pipiens*). *J Membr Biol* 155: 75–87, 1997.
15. Els WJ, Liu X, and Helman SI. Differential effects of phorbol ester (PMA) on blocker-sensitive ENaCs of frog skin and A6 epithelia. *Am J Physiol Cell Physiol* 275: C120–C129, 1998.

16. **Gommerman JL, Rottapel R, and Berger SA.** Phosphatidylinositol 3-kinase and Ca<sup>2+</sup> influx dependence for ligand-stimulated internalization of the c-Kit receptor. *J Biol Chem* 272: 30519–30525, 1997.
17. **Helman SI.** Electrochemical potentials in frog skin: inferences for electrical and mechanistic models. *Federation Proc* 38: 2743–2750, 1979.
18. **Helman SI and Baxendale LM.** Blocker-related changes of channel density. Analysis of a three-state model for apical Na channels of frog skin. *J Gen Physiol* 95: 647–678, 1990.
19. **Helman SI and Liu X.** Substrate-dependent expression of Na<sup>+</sup> transport and shunt conductance in A6 epithelia. *Am J Physiol Cell Physiol* 273: C434–C441, 1997.
20. **Helman SI, Liu X, Baldwin K, Blazer-Yost BL, and Els WJ.** Time-dependent stimulation by aldosterone of blocker-sensitive ENaCs in A6 epithelia. *Am J Physiol Cell Physiol* 274: C947–C957, 1998.
21. **Helman SI and Thompson SM.** Interpretation and use of electrical equivalent circuits in studies of epithelial tissues. *Am J Physiol Renal Fluid Electrolyte Physiol* 243: F519–F531, 1982.
22. **Koeppen BM, Beyenbach KW, Dantzer WH, and Helman SI.** Electrical characteristics of snake distal tubules: studies of I-V relationships. *Am J Physiol Renal Fluid Electrolyte Physiol* 239: F402–F411, 1980.
23. **Kurashima K, Szabó EZ, Lukacs G, Orłowski J, and Grinstein S.** Endosomal recycling of the Na<sup>+</sup>/H<sup>+</sup> exchanger NHE3 isoform is regulated by the phosphatidylinositol 3-kinase pathway. *J Biol Chem* 273: 20828–20836, 1998.
24. **Li G, D'Souza-Schorey C, Barbieri MA, Roberts RL, Klippel A, Williams LT, and Stahl PD.** Evidence for phosphatidylinositol 3-kinase as a regulator of endocytosis via activation of Rab5. *Proc Natl Acad Sci USA* 92: 10207–10211, 1995.
25. **Lindemann B and Van Driessche W.** Sodium-specific channels of frog skin are pores: current fluctuations reveal high turnover. *Science* 195: 292–294, 1977.
26. **Macchia DD and Helman SI.** Transepithelial current-voltage relationships of toad urinary bladder and colon. Estimates of E<sub>Na</sub> and shunt resistance. *Biophys J* 27: 371–392, 1979.
27. **Nakanishi S, Catt KJ, and Balla T.** A wortmannin sensitive phosphatidylinositol 4-kinase that regulates hormone sensitive pools of inositolphospholipids. *Proc Natl Acad Sci USA* 92: 5317–5321, 1995.
28. **Nakanishi S, Kakita S, Takashi I, Kawahara K, Tsukuda E, Sano T, Yamada K, Yoshida M, Kase H, and Matsuda Y.** Wortmannin, a microbial product inhibitor of myosin light chain kinase. *J Biol Chem* 267: 2157–2163, 1992.
29. **Naray-Fejes-Toth A, Canessa C, Cleaveland ES, Aldrich G, and Fejes-Toth G.** SGK is an aldosterone-induced kinase in the renal collecting duct. *J Biol Chem* 274: 16973–16978, 1999.
30. **Perkins FM and Handler JS.** Transport properties of toad kidney epithelia in culture. *Am J Physiol Cell Physiol* 241: C154–C159, 1981.
31. **Record RD, Froelich L, Vlahos CJ, and Blazer-Yost BL.** Phosphatidylinositol 3-kinase activation is required for insulin-stimulated sodium transport in A6 cells. *Am J Physiol Endocrinol Metab* 274: E611–E617, 1998.
32. **Rehn M, Weber WM, and Clauss W.** The use of kidney epithelial cell cultures (A6) in the study of Na<sup>+</sup> transport regulation. *Zool-Anal Complex Syst* 99: 221–226, 1996.
33. **Sano H, Higashi T, Matsumoto K, Melkko J, Jinnouchi Y, Ikeda K, Ebina Y, Makino H, Smedsrød B, and Horiuchi S.** Insulin enhances macrophage scavenger receptor-mediated endocytic uptake of advanced glycation end products. *J Biol Chem* 273: 8630–8637, 1998.
34. **Schild L, Canessa CM, Shimkets RA, Gautschi I, Lifton RP, and Rossier BC.** A mutation in the epithelial sodium channel causing Liddle disease increases channel activity in the *Xenopus laevis* oocyte expression system. *Proc Natl Acad Sci USA* 92: 5699–5703, 1995.
35. **Schultz SG.** Homocellular regulatory mechanism in sodium-transporting epithelia: avoidance of extinction by “flush-through”. *Am J Physiol Renal Fluid Electrolyte Physiol* 241: F579–F590, 1981.
36. **Shepherd PR, Nave BT, and O'Rahilly S.** The role of phosphoinositide 3-kinase in insulin signalling. *J Mol Endocrinol* 17: 175–184, 1996.
37. **Shepherd PR, Reaves BJ, and Davidson HW.** Phosphoinositide 3-kinases and membrane traffic. *Trends Cell Biol* 6: 92–97, 1996.
38. **Shepherd PR, Soos MA, and Siddle K.** Inhibitors of phosphoinositide 3-kinase block exocytosis but not endocytosis of transferrin receptors in 3T3-L1 adipocytes. *Biochem Biophys Res Commun* 211: 535–539, 1995.
39. **Vanhaesebroeck B, Leever SJ, Panayotou G, and Waterfield MD.** Phosphoinositide 3-kinases: a conserved family of signal transducers. *Trends Biochem Sci* 22: 267–272, 1997.
40. **Vlahos CJ, Matter WF, Hui KY, and Brown RF.** A specific inhibitor of phosphatidylinositol 3-kinase, 2-(4-morphinyl)-8-phenyl-4H-1-benzopyranol-one \*(LY294002). *J Biol Chem* 269: 5241–5248, 1994.
41. **Wu R-L, Butler DW, and Barish ME.** Potassium current development and its linkage to membrane expansion during growth of cultured embryonic mouse hippocampal neurons: sensitivity to inhibitors of phosphatidylinositol 3-kinase and other protein kinases. *J Neurosci* 18: 6261–6278, 1998.
42. **Yeh J-I, Gulve EA, Rameh L, and Birnbaum MJ.** The effects of wortmannin on rat skeletal muscle. *J Biol Chem* 270: 2107–2111, 1995.